

2022

Calculation Of Internal Flow In A Compressor With Valve Motion

Shinichi Kawabata

Ryohei Deguchi

Hideki Matsuura

Follow this and additional works at: <https://docs.lib.purdue.edu/icec>

Kawabata, Shinichi; Deguchi, Ryohei; and Matsuura, Hideki, "Calculation Of Internal Flow In A Compressor With Valve Motion" (2022). *International Compressor Engineering Conference*. Paper 2766.
<https://docs.lib.purdue.edu/icec/2766>

This document has been made available through Purdue e-Pubs, a service of the Purdue University Libraries.
Please contact epubs@purdue.edu for additional information.
Complete proceedings may be acquired in print and on CD-ROM directly from the Ray W. Herrick Laboratories at
<https://engineering.purdue.edu/Herrick/Events/orderlit.html>

Calculation of Internal Flow in A Compressor with Valve Motion

Shinichi Kawabata^{1*}, Ryohei Deguchi², Hideki Matsuura³

¹Daikin Industries, Ltd., Technology and Innovation Center,
Settsu, Osaka, Japan
shinichi.kawabata@daikin.co.jp

²Daikin Industries, Ltd., Technology and Innovation Center,
Settsu, Osaka, Japan
ryohei.deguchi@daikin.co.jp

³Daikin Industries, Ltd., Technology and Innovation Center,
Settsu, Osaka, Japan
hideki.matsuura@daikin.co.jp

* Corresponding Author

ABSTRACT

Simulation is one of the useful methods to evaluate a compressor. Simulating the flow in the compression chamber is a necessary technique to evaluate the performance and reliability of the designed compressor, and building a CFD analysis technique that can output data in three-dimensional space can capture the flow in the compression chamber more accurately. In this calculation, the compression chamber of a swing compressor is calculated by CFD, and the results of simulating the compression process are reported. The general purpose calculation code CONVERGE was used for the calculation. In this calculation, the compression chamber and the muffler space behind it were modeled. The computational space before and after the compression chamber was connected to reduce the pressure reflection generated by the calculation. The actual geometry of the discharge valve was used, and the calculation was performed using the beam behavior of the FSI. By calculating the valve behavior using the beam behavior instead of the spring-mass behavior, we thought that the behavior would be more consistent with the actual machine. As a result of the calculation, the pressure change in the compression chamber and the behavior of the discharge valve were output and compared with the results measured on the actual machine. From the comparison results, it was confirmed that the calculated results of CFD represented the characteristics of the actual machine.

1. INTRODUCTION

Compressor development is becoming more complex, requiring design based on detailed understanding of phenomena. Compressor designers are constantly examining the oil concentration ratio (Toyama, 2006), the performance (Yamamoto, 2014), and the noise and the vibration (Kikutake, 2021) to solve multiple problems, but there are some phenomena that cannot be completely explained by existing knowledge or numerical values obtained through testing alone, highly developed examination methods are required. Simulation is one such method, and is useful for deepening understanding of phenomena because it can output numerical values that cannot be measured due to the structure of the testing equipment.

This presentation describes a model building method to reproduce the refrigerant gas compression process of a swing compressor developed by CFD (Computer Fluid Dynamics) simulation. The CFD simulation was performed by comparing the pressure history and the behavior of the reed valve with the test results to see if it reproduced the trends of the test results.

In the past, Daikin Industries has developed a simulation method for swing compressors including reed valves by coupled analysis using STAR-CD. (Hori, 2009) This method reproduced test results well and was useful for simulating internal pressure changes and valve behavior depending on compressor specifications. However, this method required more than two weeks to create the model, and was not able to keep up with the recent development speedup.

While it is a prerequisite that CFD simulations can reproduce tests, reducing the study time is also important to streamline the design process. In this study, we will also discuss the results of reducing the study time by automatically creating a mesh and using the FSI (Fluid Solid Interaction) function (Pham, 2018).

2. METHODOLOGY

The mechanism of the swing compressor covered by this calculation is shown in Figure 1.

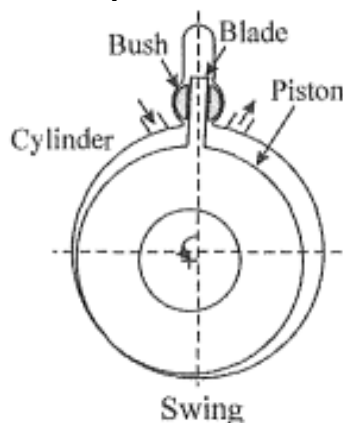


Figure 1: Swing Compressor

In swing compressors, the piston is integral with the blades and is supported by a bushing that slides between the cylinder and the blades. This feature prevents refrigerant gas leakage, which occurs between the blades and rollers in rotary type compressors. In this calculation, the piston section is modeled as a moving boundary that moves according to a given displacement, and the bushing is not modeled.

The analytical model of the swing compressor is shown in Figure 2. The computational domain was defined as the area from the inlet pipe to the muffler discharge hole. In order to suppress reflections of the pressure generated by the compression process within the computational domain, a large virtual space was connected before and after the space.

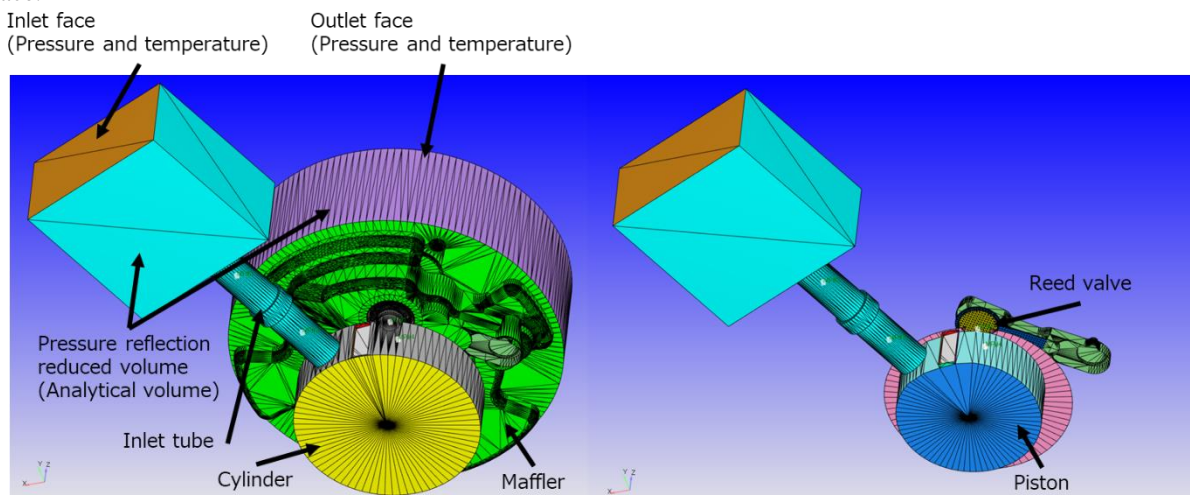


Figure 2: Analysis model

One of the reasons for selecting CONVERGE is the automatic mesh generation by cut cells. mesh generation is a process that occupies a large part of the work time in CFD simulations. In particular, the quality required of the mesh increases when the problem involves moving boundaries, such as in a compression chamber. However, it uses cut cells to create the mesh, which reduces the time required to create the mesh even for calculations with moving boundaries.

Another reason for selection is the ability to calculate reed valve behavior with FSI. The FSI function allows beam deformation to be selected, and the behavior of the reed valve can be calculated based on the discretized beam behavior. since this FSI function can also be used with cut cells, the quality requirements for the mesh are relatively low compared to other fluid analysis software.

The equation of motion for the beam model is shown in Equation (1).

$$\mathbf{M}_{ij} \frac{d^2 \mathbf{q}_i}{dt^2} + \mathbf{C}_{ij} \frac{d\mathbf{q}_j}{dt} + \mathbf{K}_{ij} \mathbf{q}_j = \mathbf{F}_i \quad (1)$$

where \mathbf{M}_{ij} is the mass matrix, \mathbf{q}_i is the beam displacement, \mathbf{C}_{ij} is the damping matrix, \mathbf{K}_{ij} is the stiffness matrix, and \mathbf{F}_i is the external force.

The mass matrix \mathbf{M}_{ij}^e is as in Equation (2).

$$\mathbf{M}_{ij}^e = \int_0^1 \rho \mathbf{A} N_i N_j d\zeta \quad (2)$$

where ρ is the density, \mathbf{A} is the cross-sectional area of the beam, and N_i and N_j are shape functions. ζ is expressed by Equation (3).

$$\zeta = \frac{2}{l^e} x - 1 \quad (3)$$

where l^e is the length of the beam element.

The stiffness matrix \mathbf{K}_{ij}^e is as in Equation (4).

$$\mathbf{K}_{ij}^e = \int_0^1 EI \frac{dN_i}{d\zeta} \frac{dN_j}{d\zeta} d\zeta \quad (4)$$

where E is Young's modulus and I is the sectional second moment.

The force vector \mathbf{F}_i^e is as in Equation (5).

$$\mathbf{F}_i^e = \int_0^1 \mathbf{f} N_i d\zeta \quad (5)$$

where \mathbf{f} is the force per unit length applied to the beam.

The attenuation force \mathbf{C}_{ij}^e is expressed by Equation (6).

$$\mathbf{C}_{ij}^e = \mathbf{C}_k \mathbf{K}_{ij}^e + \mathbf{C}_m \mathbf{M}_{ij}^e \quad (6)$$

where \mathbf{C}_k and \mathbf{C}_m are damping coefficients and are specified as inputs to the calculation. In this report, \mathbf{C}_k is set to 0 and \mathbf{C}_m is adjusted.

When performing a coupled fluid/structure calculation using a beam, it takes the displacement of the structure from the previous calculation step and uses it as the new boundary condition, and the structure is calculated with the fluid force as the external force. This is repeated to calculate the deformation of the beam due to the fluid.

In this calculation, a porous material is given between the piston and the cylinder. The porous material is automatically inserted when the distance between the piston and cylinder is small. The porous media simulates a seal by oil in the compression chamber. The resistance provided by the porous media is shown in Equation (7).

$$-K_i u_i = \frac{\partial p}{\partial \xi_i} \quad (7)$$

where K_i is the resistivity, u_i is the apparent flow velocity in the direction of ξ_i , and p is the pressure. The resistivity K_i is expressed by Equation (8).

$$K_i = \alpha_i |v_i| + \beta_i \quad (8)$$

Here, α_i and β_i are user-input coefficients and $|v_i|$ is the magnitude of the apparent velocity. The degree of leakage at the seal was adjusted by adjusting these α_i and β_i . In this report, 1.0E8 was used for both α_i and β_i .

The following table shows the calculation conditions for this report. The calculations were performed under two conditions: 28 rps and 110 rps.

Table 1: Analysis condition

| Rotational speed | 28rps | 110rps |
|------------------|----------|----------|
| Tc | 27°C | 45°C |
| Te | 3°C | -7°C |
| Hp | 1.78 MPa | 2.79 MPa |
| Lp | 0.89 MPa | 0.65 MPa |

3. RESULTS AND DISCUSSION

3.1 Adjustment of Damping Factor Cm for 28 rps Conditions

The internal pressure and valve lift output from the CFD simulation are shown in Figure.3. First time, the damping coefficient Cm was matched with a calculation of 28 rps, and the sharp increase in internal pressure around 310° is due to the sealing area of the porous material in the calculation model crossing the internal pressure monitoring point.

The results show good agreement in the frequency of the re-expansion pulsation during compression and the internal pressure behavior after over-compression and valve opening. The behavior of the reed valve also varies in terms of maximum lift and before valve closure, but the trend is well captured. 110 rps valve behavior has a higher peak value for the lift behavior at the beginning of the valve opening than the actual measurement.

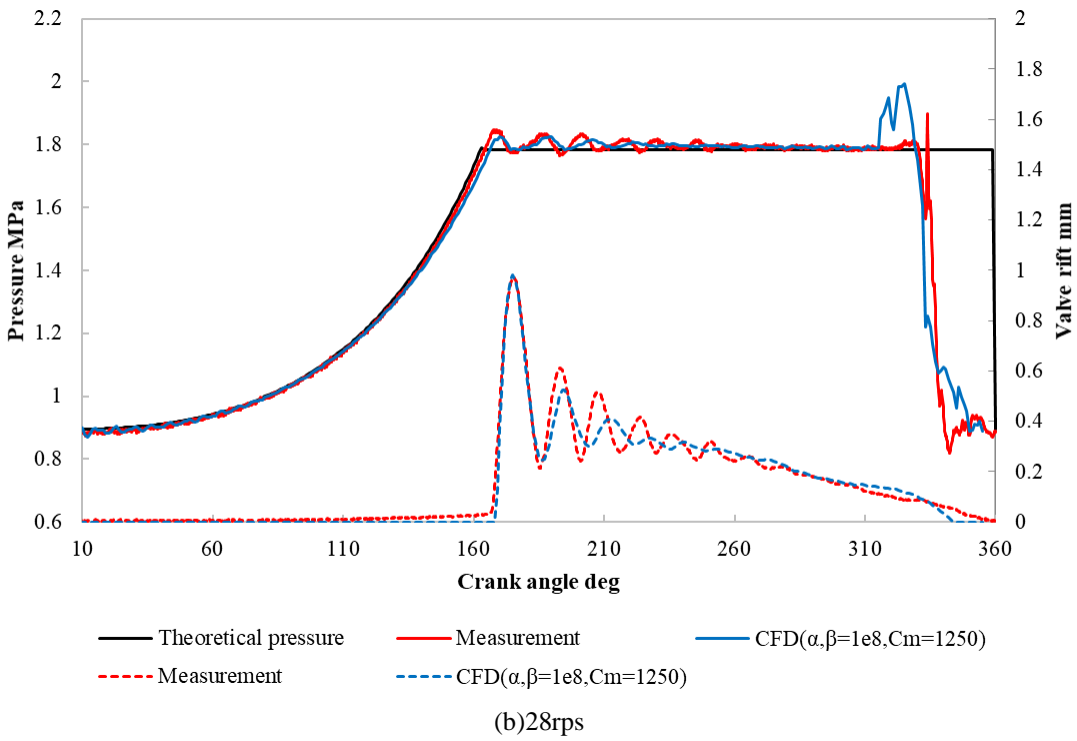
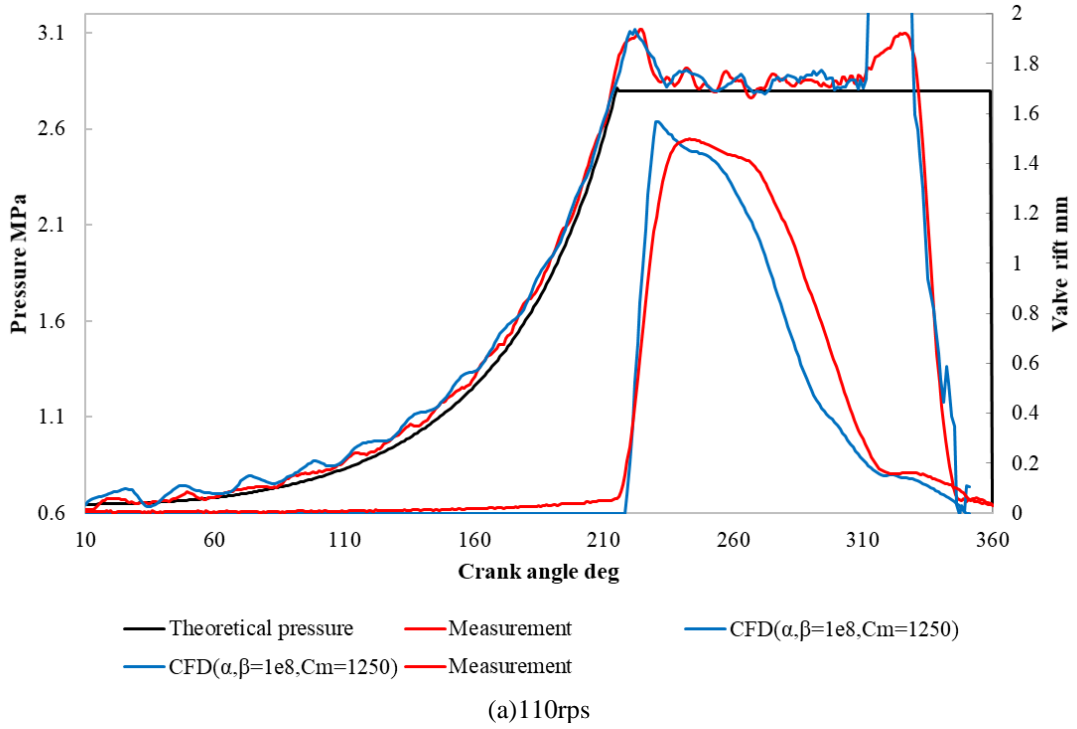


Figure 3: Pressure curve and valve rift (Fitted Cm Factor for 28rps)

3.2 Adjustment of Damping Factor C_m for 110 rps Conditions

Regarding the valve behavior at 110 rps having a larger peak than the test results, the damping factor C_m of the valve behavior was adjusted to 110 rps to correct the deviation from the test results.

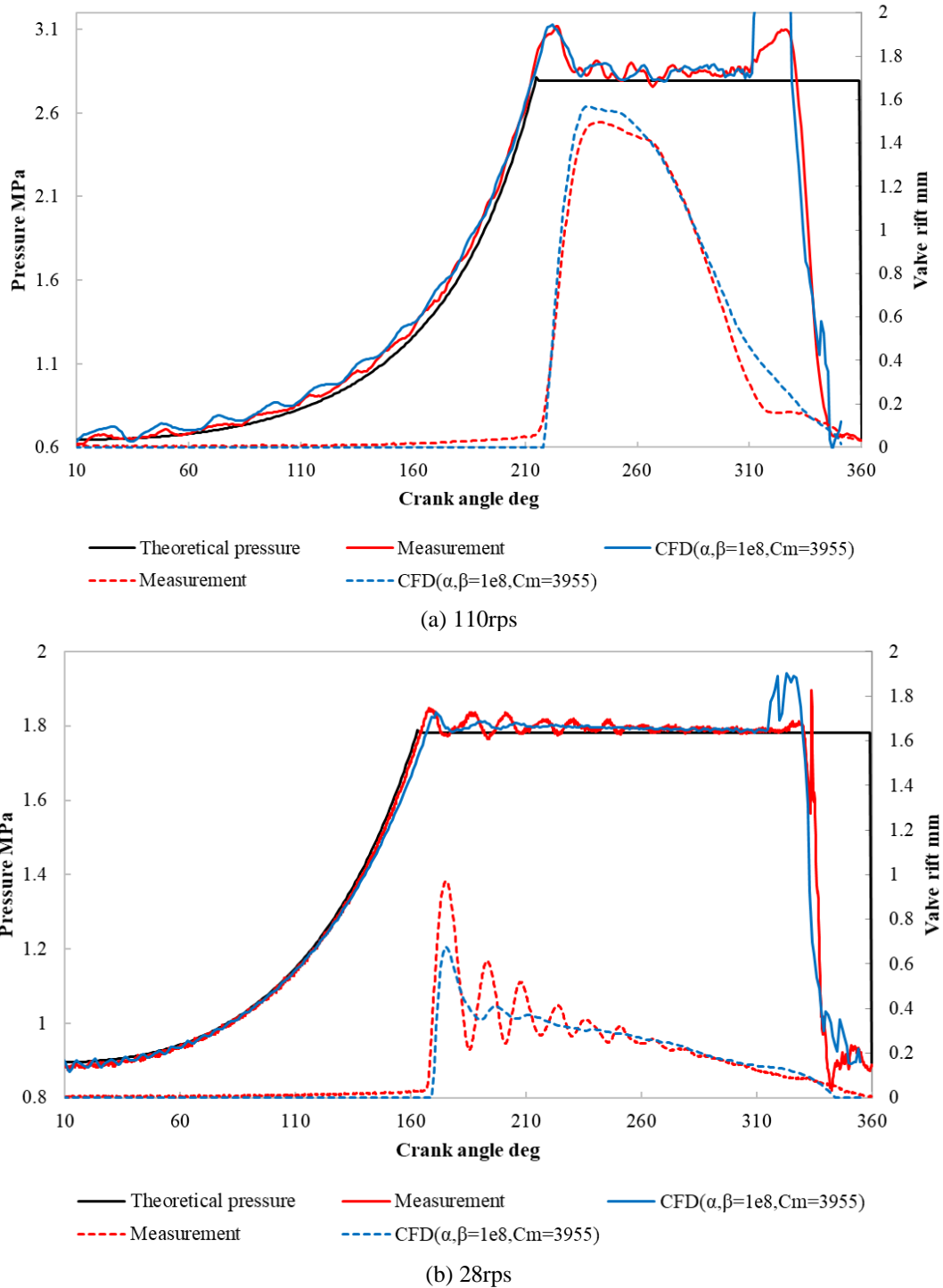


Figure 4: Pressure curve and valve rift (Fitted C_m Factor for 110rps)

It was found that adjusting the damping factor C_m to 110 rps brought the valve behavior closer to the actual measurement. However, at 28 rps, the valve behavior changed in a direction that deviated from the actual measurement, and internal pressure leakage was also found to occur.

The coefficient of C_m is considered to be rotational speed dependent in the calculation of the swing compressor.

3.3 Adjustment of Damping Factor C_m and Porous Coefficients α and β for 110 rps

Adjustments were made to the porous media coefficient and C_m . The results of the parameter adjustments are shown in Figure.5.

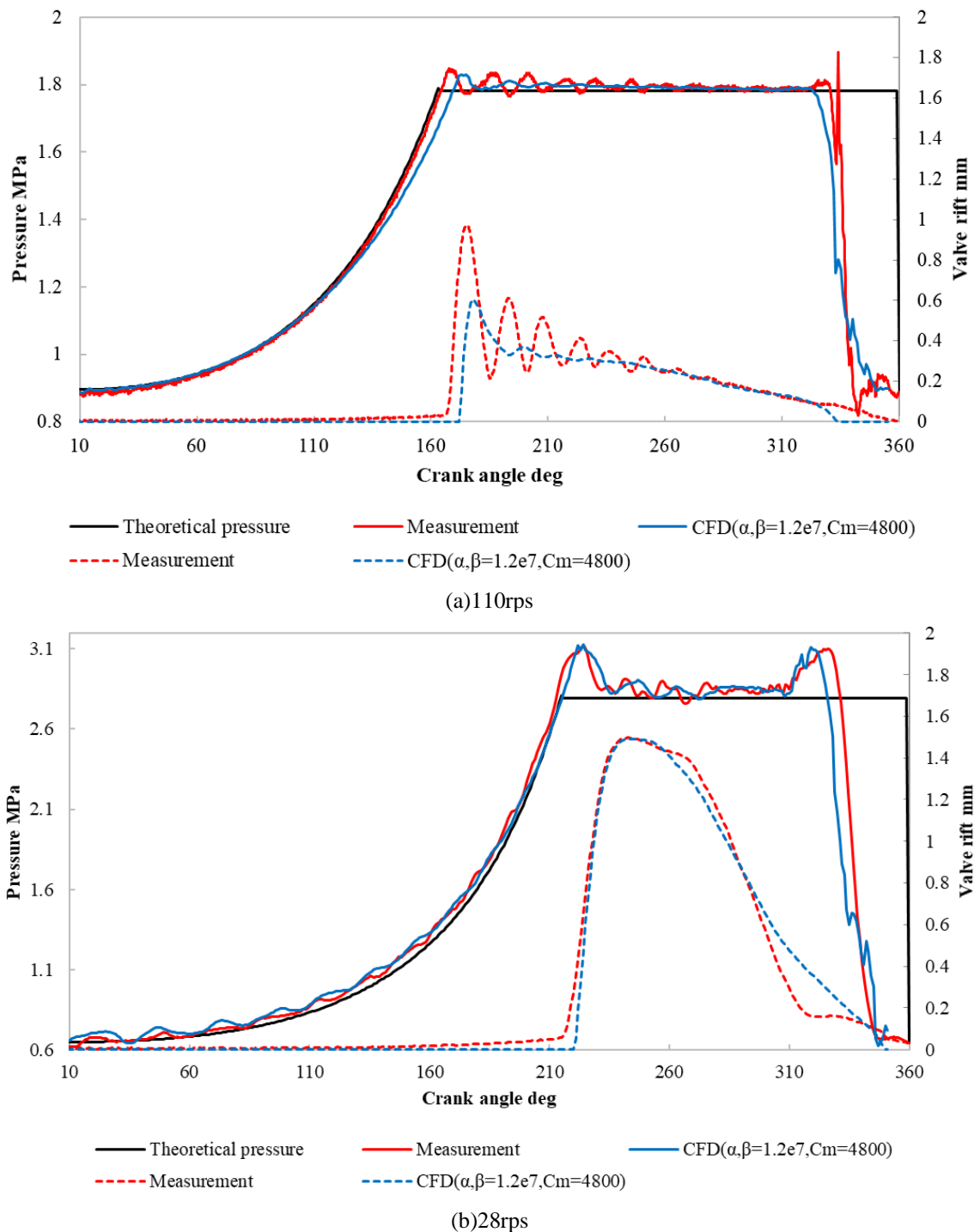


Figure 5: Pressure curve and valve rift (Control C_m and porous factor Factor for 110 rps)

The valve lift at 110 rps tended to agree well, including the maximum value, and the sudden pressure increase caused by the porous media, which occurred around 310°, was also suppressed. However, calculations at 28 rps deviated more from the test results, mainly in terms of valve behavior.

From the above discussion, it was found that adjusting the coefficient of porous material together with C_m can better reproduce the test results. On the other hand, since the parameters are not applicable when the rotation speed changes, it is necessary to construct a method to select the porous media coefficient together with C_m in a manner that depends on the rotation speed.

3.4 Shortening the Time of Analysis

The CFD simulations reported in this report have resulted in significant time savings compared to the lead valve calculations conducted in the past. The conventional simulation took two weeks to create the mesh, but by using this analysis method, the mesh creation man-hours were reduced to zero. In addition, the computation time itself for all of the calculations presented in this report is only a few hours to half a day, which is not an increase in computation time compared to the conventional method. Rather, at high rotation speed, the calculation time can be significantly reduced. In the field of design and development, where high speed is required, a time reduction of two weeks or more is a significant effect.

4. CONCLUSIONS

Calculations of the compression process, including the swing compressor reed valve, were performed using CONVERGE. The calculated internal pressure agreed well with the test results. For the reed valve, it was found that the valve behavior in the experiment could be simulated by adjusting the damping factor C_m . The porous material coefficient was also found to have a significant influence on the calculation results, and it is necessary to develop a method to uniquely determine the coefficient of the calculation model together with C_m in the future.

Regarding the reduction of calculation time, a significant time reduction of more than two weeks was achieved compared to the existing study method. In addition, the calculation results were equivalent to those of the conventional method, confirming that the use of this analysis method is useful for speeding up the design study.

In the future, we will examine how to handle oil and phase change phenomena that have not yet been modeled in the design and development process, as well as conduct calculations using different models to verify accuracy.

REFERENCES

- Toyama, T., Matsuura, H. and Yoshida, Y. (2006), Visual Techniques to Quantify Behavior of Oil Droplets in a Scroll Compressor, *International Compressor Engineering Conference at Purdue*, (Paper C026)
- Kikutake, D., Katayama, T., Matsuura, H. (2021), Theoretical Analysis of Rigid-Body Vibration in Swing Compressors, *25th International Compressor Engineering Conference at Purdue*, (Paper 1174)
- Yamamoto, Y., Kanayama, T., Yuasa, K., Matsuura, H. (2014), Development of High Efficiency Swing Compressor for R32 Refrigerant, *International Compressor Engineering Conference at Purdue* (Paper 1286)
- Hori, K. (2009), Investigation on Fluid Phenomenon of Air-Conditioning Compressors using Fluid-Structure Coupling Analysis, *JSRAE Annual Conference*, (Paper B313)
- Pham, H. D., Brandt, T., Rowinski, D. H. (2018), Modeling A Scroll Compressor Using A Cartesian Cut-Cell Based CFD Methodology With Automatic Adaptive Meshing, *24th International Compressor Engineering Conference at Purdue*, (Paper 1252)